Identification of Anti-Inflammatory Components from *Launaea sarmentosa* Using *In Vitro* Cell Model

Thanh Quoc Chau Nguyen[1*], Khang Thanh Vo[1,2], Cua Dinh Duong[1,2], Toan Phu Huynh[1,2], Lieu Thi Thuy Ca[2], and Giao Huynh Dang[3]

[1]*Department of Chemistry, College of Natural Sciences, Can Tho University, Campus II, 3/2 Street, Can Tho 94000, Vietnam*

[2]*Medicinal Chemistry Laboratory, CTU Hi-tech Building, Can Tho University, Campus II, 3/2 Street, Can Tho 94000, Vietnam*

[3]*College of Engineering, Can Tho University, Campus II, 3/2 Street, Can Tho 94000, Vietnam*

* ***Corresponding author:***

tel: +84-909-747547
email: nqcthanh@ctu.edu.vn

Received: December 28, 2024
Accepted: April 29, 2025

DOI: 10.22146/ijc.103167

Abstract: Launaea sarmentosa *(Willd.) Kuntze, a medicinal herb known for treating inflammatory diseases, was examined for its anti-inflammatory compounds to identify novel therapies. This study indicated that hexane and ethyl acetate fractional extracts significantly reduced NO secretion in LPS-stimulated RAW264.7 macrophages, indicating the presence of potential anti-inflammatory compounds. Additionally, four anti-inflammatory compounds, including taraxasteryl acetate (1), esculetin (2), pyrimidine-2,4-dione (3), and 5-hydroxypyrrolidin-2-one (4), were isolated, and their structures were characterized using 1D and 2D-NMR. This study marked the first report of taraxasteryl acetate, pyrimidine-2,4-dione, and 5-hydroxypyrrolidin-2-one being isolated from this species. Furthermore, these compounds exerted their anti-inflammatory role by inhibiting NO production and TNF-α expression. Thus, this study contributes to identifying anti-inflammatory constituents from* L. sarmentosa *and highlights a potential approach for developing phytotherapeutic agents.*

Keywords: *anti-inflammatory; Asteraceae;* Launaea sarmentosa*; isolation; RAW264.7 macrophages*

■ INTRODUCTION

Launaea sarmentosa (Ls), part of the Asteraceae family, is a valued medicinal herb recognized for its diverse therapeutic benefits. In Vietnam, Ls has been domesticated and is extensively cultivated. Traditionally, Ls is celebrated for its strong medicinal qualities, particularly in treating coughs, expelling phlegm, and lowering fevers [1-3]. Previous studies on Ls have identified several bioactive compounds, including polyphenols, flavonoids, saponins, alkaloids, tannins, and steroids [4]. Moreover, Ls exhibits significant antibacterial, antioxidant, and hepatoprotective activities [2,5-6]. Besides, methanol extracts have shown potent inhibition of proinflammatory cytokines [2,7]. However, the specific natural compounds responsible for its anti-inflammatory effects have yet to be thoroughly investigated. This also restricts the availability of effective inflammatory therapies.

Inflammation is a crucial immune system defense mechanism, responding to infection or irritation. While it is vital for healing and protection, chronic inflammation can contribute to the development and progression of various diseases, including diabetes, cancer, and Alzheimer's diseases [8-9]. Macrophages are key contributors to the inflammatory response, controlling the release of cytokines, chemokines, and various other inflammatory mediators [10-11]. Among these, nitric oxide (NO), prostaglandin E2 (PGE2), interleukin-6 (IL-6), and tumor necrosis factor-alpha (TNF-α) are especially important [12]. Inducible nitric oxide synthase (iNOS) catalyzes the NO production in macrophages, hepatocytes, and renal cells, and its activation is triggered by stimuli such as

lipopolysaccharide [13]. Excessive NO production is strongly implicated in the pathogenesis of various inflammatory disorders, including sepsis, inflammation-induced tissue damage, and rheumatoid arthritis [14-16]. Excessive NO production is a characteristic of the inflammatory response, contributing to both its protective and harmful effects. As a result, tracking changes in NO levels is crucial for assessing the effectiveness of anti-inflammatory compounds [15,17]. Collectively, to devise new strategies for drug development and gain a comprehensive understanding of the potential of natural products, this study further explores anti-inflammatory constituents from Ls using RAW264.7 macrophage cells in LPS stimuli.

■ EXPERIMENTAL SECTION

Materials

L. sarmentosa (Ls) was harvested in Ben Tre province, Vietnam, in August 2022. The specimen of Ls was botanically authenticated by Assoc. Prof. Dang Minh Quan and stored under specimen code VNM00082022CTU of Nation Plant Resources Center, Vietnam. All chemical reagents, including dimethyl sulfoxide (DMSO), Dulbecco's Modified Eagle Medium (DMEM), and penicillin-streptomycin, were purchased from Sigma-Aldrich, Germany, except Griess-reagent, Lipopolysaccharide (LPS), N-Nitro-L-arginine methyl ester (L-NAME) from FUJIFILM-Wako, Japan; Trizol reagent from Invitrogen, Cell Counting Kit-8 assay (CCK-8) from Dojindo Molecular Technologies Inc., and Fetal Bovine Serum (FBS) from Hyclone, USA; Qiagen RNeasy Kit from Qiagen, Transcriptor Universal cDNA Master Mix and FastStart Essential DNA Green Master Mix from Roche, Germany. For the extraction and isolation process, solvents such as acetone, methanol, ethanol, *n*-hexane, ethyl acetate, dichloromethane, and chloroform were used in this research from Xilong, China.

Instrumentation

Following the extraction process, a waring two-Speed laboratory blender (Cole-Parmer, USA), Elmasonic S100H ultrasonic water bath (Elma, Germany), and rotavapor R300 (BUCHI, Switzerland) were used as the initial step for preparing crude extract. Biotek Epoch microplate reader (BioTek, USA) was used to evaluate the bioactivity. SimpliAmp™ Thermal Cycler (Life Technologies, Singapore) and Light-Cycler 96 (Roche, Germany) were applied for RT-*q*PCR assay. For experimental analysis, thin layer chromatography (TLC, precoated aluminum silica gel plate 60-F_{254} or RP-18 F_{254}) and silica gel 60 particle size 0.04–0.063 mm were obtained from Merck, Germany. Fourier transform infrared (FTIR) data were conducted by FT/IR-6700 (Jasco, Japan). Besides, all spectra data of 1D and 2D-nuclear magnetic resonance (NMR) were measured using Bruker Avance III-600 MHz (Bruker, Rheinstetten, Germany) at the Kyoto Institute of Technology (Kyoto, Japan) and Vietnam Academy of Science and Technology (Ha Noi, Vietnam).

Procedure

Extraction and isolation

The aerial part of Ls was carefully checked, the root and soil were removed, and then washed under tap water and dried at 55 °C in an oven without light. The sample was then ground using a blender to obtain a dry powder and kept at −20 °C for further extraction. The moisture content of the dried sample was recorded as 5.08 ± 0.99%. The crude extract of Ls was obtained using an ultrasound-assisted extraction method. Briefly, 1 kg of dried powder was separated, added to a small bag, and then soaked directly into methanol (e.g, a ratio of solvent-to-material, 21 mL/g) under an ultrasound frequency of 37 kHz and 500 W nominal power according to the optimal extract process. Next, all supernatants were combined, filtered, and concentrated using Rotavapor R300 to obtain the crude extract (126.7 g), yielding 12.67%. The crude extract was stored at 4 °C for further investigation.

An amount of 100 g crude extract was partitioned in ascending order of polarity solvents, resulting in 24.6 g of *n*-hexane fraction (Hex-frc), 8 g of ethyl acetate fraction (EtOAC-frc) and 12.4 g of aqueous fraction (Aq-frc), respectively. According to the initial step of isolation process, the *n*-hexane fraction was subjected to normal-phase column chromatography, then eluted

with gradient of *n*-hexane, ethyl acetate and methanol (Hex:EtOAc:Me, 100:0:0–0:0:100), producing 18 sub-fractions based on TLC analysis, as numbered H.1–H.18. Here, sub-fraction H.2 (3.2 g) was repeatedly purified using *n*-hexane to obtain compound **1** (formed a colorless oily wax, 2.5 mg). Besides, the ethyl acetate fraction was similar subjected and eluted with Hex:EtOAc:Me (100:0:0–0:0:100), yielding 10 sub-fractions (E.1–E.10). Sub-fractions E.3 (3.54 g) was divided into 4 small sub-fractions which assigned as E.3.1–E.3.4. Compound **2** (formed amorphous pale yellow powder, 7 mg) was isolated from sub-fraction E.3.2.3 using chloroform.

Similarly, sub-fraction E.6 (5.88 g) was repeatedly purified with a gradient of Hex:EtOAc:Me (100:0:0 to 0:0:100) to afford 4 small sub-fractions (E.6.1–E.6.4). TLC analysis of sub-fraction E.6.2 (520 mg) confirmed the presence of compound **3**, which was then isolated by column chromatography by eluting with *n*-hexane and ethyl acetate (75:25). After the separation, compound **3** was recovered as 9 mg of white crystalline. Besides that, sub-fraction E.6.3 was also separated with the increasing of polarity solvents (EtOAc:Me, 100:0 to 0:100) to obtain 3 small sub-fractions (E.6.3.1–E.6.3.3). Among sub-fraction E6.3.2, a single orange-yellow spot appeared in TLC but contained impurities, then was purified twice time by a gradient solvent of chloroform: methanol (96:4), resulting in compound **4** (formed colorless crystals, 3.7 mg).

Compound 1, colorless oily wax. ^{1}H-NMR (600 MHz, $CDCl_3$, δ, ppm, *J*/Hz): 4.62 (1H, *dd*, *J* = 1.8 & 7.8 Hz, H-3), 4.50 (2H, *m*, H-30), 2.47 (1H, *m*, H-21a), 2.22 (1H, *m*, H-21b), 2.10 (1H, *m*, H-19), 2.04 (3H, *s*, H-1), 1.73 (*m*, H-1), 1.70 (*m*, H-12a), 1.69 (*m*, H-2), 1.67 (*m*, H-15a), 1.63 (*m*, H-13), 1.55 (*m,* H-6, H-11), 1.42 (*m*, H-7), 1.37 (*m*, H-9), 1.26 (*m*, H-16a), 1.16 (*m*, H-12b, H-16), 1.05 (*s*, H-26), 1.032 (*d*, *J* = 6.6 Hz, H-29), 1.00 (*m*, H-18), 0.97 (*s*, H-15b), 0.95 (*s*, H-27), 0.93 (*s*, H-25), 0.88 (*s*, H-23), 0.86 (*d*, *J* = 7.2 Hz, H-5), 0.85 (*s*, H-28), 0.84 (3H, *m*, H-24). ^{13}C-NMR (150 MHz, $CDCl_3$, δ, ppm): 171.0 (C-1'), 154.7 (C-20), 107.1 (C-30), 81.3 (C-1), 55.5 (C-5), 50.5 (C-9), 48.7 (C-18), 42.1 (C-14), 41.0 (C-8), 39.4 (C-19), 39.2 (C-13), 38.9 (C-22), 38.5 (C-1), 38.3 (C-16), 37.8 (C-4), 37.1 (C-10), 34.6 (C-17), 34.1 (C-7), 28.0 (C-23), 26.7 (C-15), 26.2 (C-12), 25.7 (C-21), 25.5 (C-29), 23.7 (C-2), 21.5 (C-11), 21.3 (C-2'), 19.5 (C-28), 18.2 (C-6), 16.5 (C-24), 16.4 (C-25), 15.9 (C-26), 14.8 (C-27).

Compound 2, amorphous pale yellow powder. ^{1}H-NMR (600 MHz, DMSO-d_6, δ, ppm, *J*/Hz): 7.86 (1H, *d*, *J* = 9.6 Hz, H-3), 6.78 (1H, *s*, H-5), 6.74 (1H, *s*, H-8), 6.16 (1H, *d*, *J* = 9.6 Hz, H-4). ^{13}C-NMR (150 MHz, DMSO-d_6, δc ppm): 160.7 (C-2), 150.4 (C-7), 148.5 (C-6), 144.4 (C-4), 142.8 (C-9), 112.3 (C-5), 111.5 (C-3), 110.7 (C-10), 102.6 (C-8).

Compound 3, white crystals. ^{1}H-NMR (600 MHz, DMSO-d_6, δ, ppm, *J*/Hz): 11.04 (2H, *brs*, H-1 & H-3), 7.36 (1H, *d*, *J* = 7.6 Hz, H-6), 5.49 (1H, *d*, *J* = 7.6 Hz, H-5). ^{13}C-NMR (150 MHz, DMSO-d_6, δc ppm): 166.2 (C-4), 153.0 (C-1), 143.8 (C-6), 101.7 (C-5).

Compound 4, colorless crystals. ^{1}H-NMR (600 MHz, CD_3OD, δ, ppm, *J*/Hz): 5.17 (1H, *dd, J* = 6.6 & 1.2 Hz, H-5), 2.48 (2H, *m, J* = 16.8, 9.6 & 3.0 Hz, H-3a), 2.37 (2H, *m,* H-4a), 2.19 (2H, *m,* H-3b), 2.03 (2H, *m,* H-4b). ^{13}C-NMR (150 MHz, CD_3OD, δ, ppm): 181.4 (C-2), 85.3 (C-5), 29.8 (C-4), 29.2 (C-3).

Cytotoxicity assay

RAW264.7 macrophages, a density of 2×10^5 cells/well, were seeded in a 96-well plate in DMEM (ingredients included 10% FBS, 1% L-glutamine, and penicillin-streptomycin) and then incubated at 37 °C, 95% humidity, 5% CO_2. Next, cells were immersed in a medium, followed by the addition of samples at various concentrations of extract (50, 100, 200, 400 μg/mL) or compounds (0–16 μg/mL) for 24 h, and stimulated in the presence of LPS (1 μg/mL) for 18 h. Subsequently, the medium was removed, washed twice with phosphate buffer saline (PBS), and 100 μL CCK-8 was added according to the manufacturer's instructions. Finally, the absorbance was recorded at 450 nm using a microplate reader, as described in a previous report [2].

Nitric oxide inhibitor assay

Cells were similarly cultured in a 24-well plate under the conditions above, following LPS-stimulated for 18 h. NO secretion was assessed to evaluate the efficiency of each sample (e.g., a safe concentration of 200 μg/mL for extract or 0–4 μg/mL of isolated compounds) under LPS-induced inflammation [2].

Briefly, an equal volume of cell supernatant and Griess reagent was incubated without slight at room temperature within 10 min. The absorbance was measured at the wavelength of 540 nm. The NO concentration was determined according to the $NaNO_2$ calibrate curve ($y = 0.0034x + 0.0093$; $R^2 = 0.9992$) in comparison with negative control as only culture medium without LPS and positive control as N-Nitro-L-arginine methyl ester (L-NAME, 100 μM).

Real-time qPCR assay

Cells were cultured in a 6-well plate and then incubated within purified compounds at 4 μg/mL in the presence of LPS (1 μg/mL). Subsequently, total RNA was extracted and purified using Trizol and Qiagen RNeasy Kit, respectively, according to the manufacturer's instructions, and then stored at −80 °C for further analysis. mRNA was converted into cDNA using a SimpliAmp™ Thermal Cycler. After that, the polymerase chain reaction in the mixture of cDNA sample and specific primes was quantified using FastStart Essential DNA Green Master Mix and Light-Cycler 96. β-actin, as a standard housekeeping gene for normalizing control. All primers were used in this experiment, as mentioned in Table S1.

Data analysis software

All experiments were performed in triplicate, and the results were stated as mean ± standard deviation (SD) using ANOVA with GraphPad Prism 8.0.1 software (GraphPad Software Inc., USA).

■ RESULTS AND DISCUSSION

Evaluation of Cytotoxicity and Anti-Inflammatory Activity

Prior to the isolation of anti-inflammatory compounds, the cytotoxicity and the inflammatory suppression were initially investigated to evaluate the effect of Ls extract and its fraction their extract on LPS-stimulated macrophages. Preliminary evaluation results indicated that the cell survival of Ls and its fraction was not significantly changed in comparison with the control group at 200 μg/mL, presenting a safe concentration for further experiments. While LPS-activated macrophages could enhance cell damage, as formed apoptosis and pyrosis, easily observed via morphological cell changing, co-incubating these fractions with LPS could improve cell viability (data not shown) [17]. These results were in accordance with our previous study that stated Ls extract and its fraction could protect macrophages against LPS-induced cell damage [2].

NO plays an important role as a toxic defense signaling molecule against infectious organisms, related to many aspects of immunomodulation and inflammation response [14-15]. Indeed, removing NO excess was demonstrated to improve abnormally high NO secretion in hepatic failure and sepsis [18]. Here, NO-releasing since LPS-incubated was higher in comparison with a control group, reaching a concentration up to 89.91 μM; whereas this value was at 22.66 μM in the absence of LPS (Table S2). Obviously, NO production increased markedly during LPS-stimulated macrophages, indicating one of the immune manifestations in response to inflammation after infection [19]. Additionally, the reference control of L-NAME, as a commercial inhibitor of NOS, significantly reduced NO secretion (75.3 μM of NO concentration). Notably, co-incubation with Ls crude extract and its fraction also suppressed the NO level from LPS-stimulated macrophages following the order of EtOAc-frc (64.52 μM), Hex-frc (68.17 μM), Ls crude extract (71.77 μM) and Aq-frc (72.85 μM), respectively. It is also worth noting that the NO inhibition observed may be attributed to non-polar and moderately polar compounds, such as flavonoids and terpenoid groups, identified during fractionation steps. Hence, EtOAc-frc and Hex-frac were chosen to isolate active compounds, and their efficacy in inflammation response was assessed.

Anti-Inflammatory Effect of Active Compounds

Concerning the presence of anti-inflammatory ingredients, all isolated compounds were investigated the cytotoxicity with and without LPS-stimulated on RAW264.7 cells. Among these compounds isolated from Hex-frac and EtOAC-frac, compound **1** was in minimal quantities, which was inadequate for bioassay. Consequently, compounds **2**, **3**, and **4** were selected to

investigate their anti-inflammatory effects in greater detail further.

As illustrated in Fig. 1(a), there is no cytotoxicity up to 8 μg/mL for the incubation group compared to the non-incubated compounds, except compound **2**. Besides, in the presence of LPS, a similar trend was observed, as noted that the percentage of cell survival reduced by about 20% at 8 μg/mL of compound **2** (Fig 1(b)). Obviously, in terms of macrophage morphology, cells from LPS-stimulated exhibited shrinkage, cell membrane rupture, and cell death, resulting in a decreased cell density (Fig. 2(b)) [2,20]. Notably, cells pretreated with compounds **3** and **4** retained their original round shape despite LPS stimulation at 8 μg/mL (Fig. 2(d) and 2(e)). Conversely, compound **2** demonstrated higher toxicity, causing abnormal cell deformation, indicating significant cytotoxic effects at similar conditions (Fig. 2(c)). This could improve the hypothesis that the existence of these compounds is not only non-cytotoxic but also offers protection against LPS-induced cellular damage.

Regarding the expression of proinflammatory mediators, the NO level was reliably employed to evaluate the effect of the active ingredients under LPS-induced inflammation. As expected, pretreatment with compounds **2**, **3**, and **4** markedly suppressed NO production (Fig. 3). This observation pointed out that these compounds exhibited anti-inflammatory properties; however, the toxicity at higher concentrations might be causing the limitation of their therapeutic application. These findings illustrated that these compounds effectively inhibited the production of inflammatory mediators, for example, NO, in LPS-stimulated RAW264.7 macrophages while maintaining non-toxic concentrations.

To enhance the evidence for the anti-inflammatory activity of these compounds, the level of proinflammatory

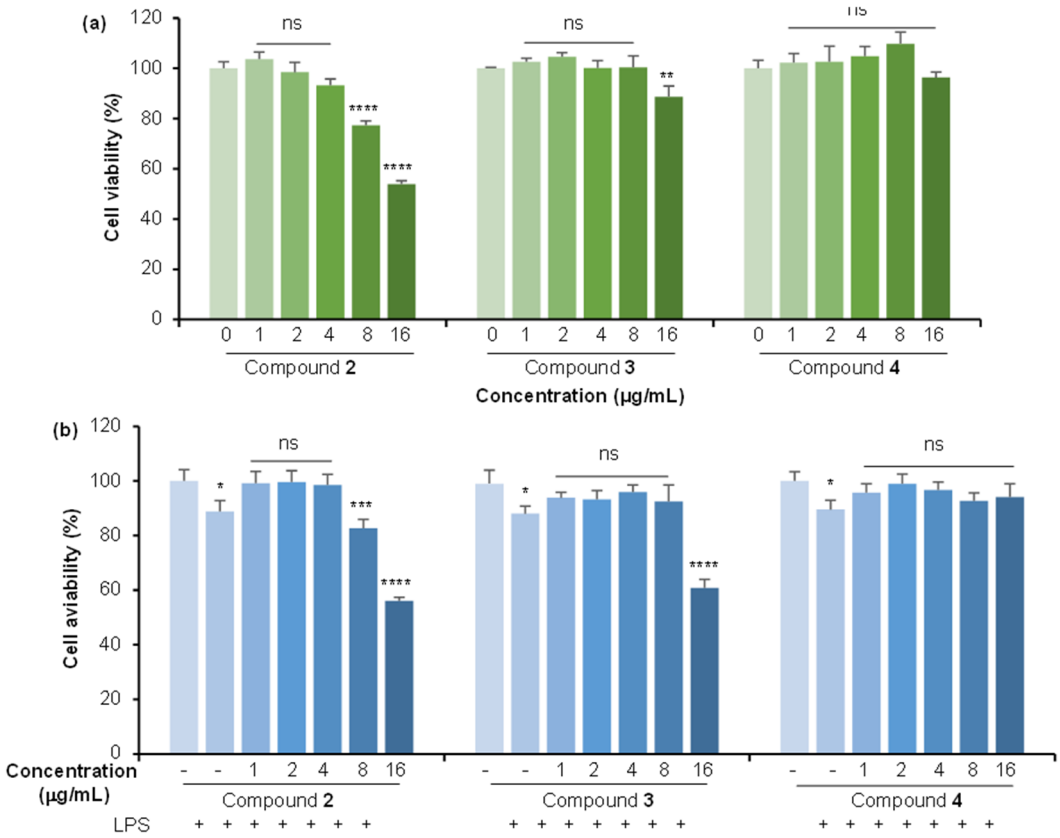

Fig 1. Cytotoxicity of compounds in the presence (a) and absence (b) of LPS-stimulated RAW264.7 cell. Data are presented as mean ± S.D (n = 6); *, *p*-value < 0.05; ***, *p*-value < 0.001; ****, *p*-value <0 .0001 vs. cell was treated with medium; ns: non-significant

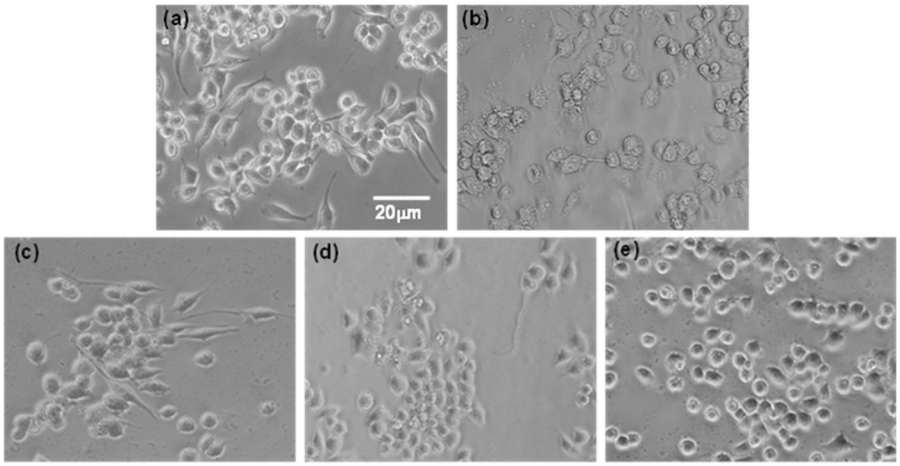

Fig 2. The cell morphology in the presence of compounds (8 μg/mL) was observed under LPS-incubated. (a) Cell was treated with medium only; (b) cell was incubated with LPS; (c) cell was pretreated with compound **2**, followed by LPS; (d) cell was pretreated with compound **3**, followed by LPS; and (e) cell was pretreated with compound **4**, followed by LPS

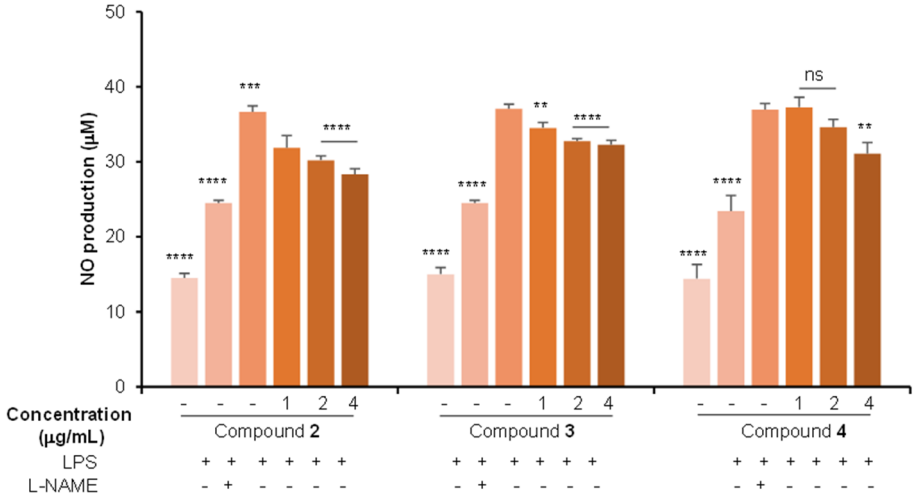

Fig 3. Effects of compounds **2**, **3**, and **4** on NO production under LPS stimulation. Data are presented as mean ± S.D (n = 6); **, *p*-value < 0.01; ***; *p*-value < 0.001; ****, *p*-value < 0.0001 vs. LPS-treated group; ns: non-significant

cytokine, such as TNF-α, was investigated using *q*RT-PCR. TNF-α is one of the central cytokines produced by the immune system that directly promotes inflammatory reactions and indirectly induces cell death [21]. Moreover, TNF-α regulates NOS expression, influencing NO secretion and the homeostatic environment of vascular endothelial cells [22]. As illustrated in Fig. 4, adding compounds **2**, **3**, and **4** significantly suppressed the mRNA expression of TNF-α by 2.1, 1.3, and 3.0-fold, respectively, while LPS caused overexpression of TNF-α level. Compound **4** exerted the highest adequate compared to other compounds. Hence, these results indicated that the existence of active ingredients might alleviate the expression of proinflammatory mediators, suggesting their protective role against infection.

Identification of Compounds

The structures of four compounds isolated from Ls were elucidated by analyzing 1D, 2D-NMR, and MS spectroscopic data and by comparison with the previously reported spectral data (Fig. 5). The ^{1}H-NMR spectrum of this compound displayed characteristic signals indicative

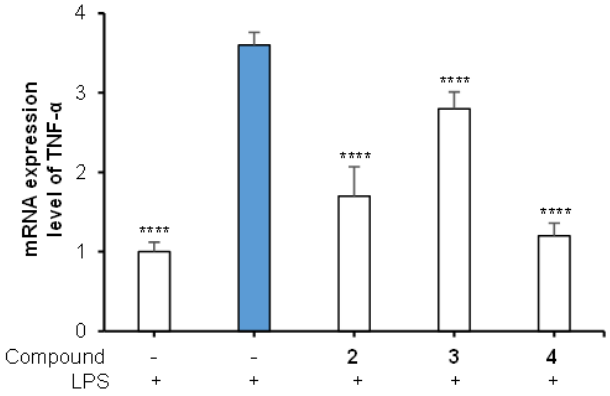

Fig 4. Effects of isolated compounds (4 µg/mL) on mRNA TNF-α level under LPS stimulation. Data are presented as mean ± S.D (n = 4); ***, *p*-value < 0.001; ****, *p*-value < 0.0001 vs. LPS-treated group

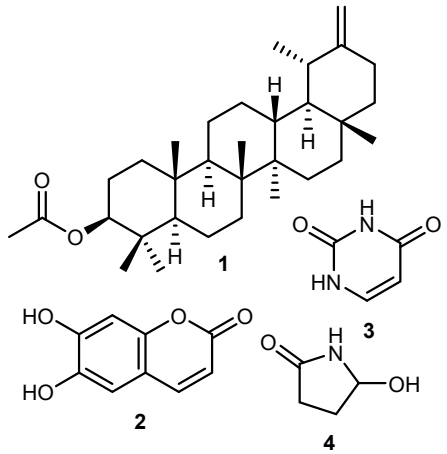

Fig 5. Chemical structure of compounds **1**–**4** isolated from *L. sarmentosa*

of triterpenes. Specifically, methyl group signals were observed at δ_H 0.84, 0.83, 0.86, 0.88, 0.93, 0.95, and 0.97 ppm (Fig. S1–S5). Additionally, a distinct singlet at δ_H 2.04 (3H, *s*) suggested the presence of an acetyl group within the molecule. The ^{13}C-NMR spectrum further corroborated this structure, showing 32 distinct carbon resonances, including two olefinic carbons at δ_C 154.7 and 107.1 ppm, which are characteristic of a double bond in a taraxerane skeleton. Moreover, the ^{13}C-NMR spectrum revealed a signal at δ_C 171.0 ppm, corresponding to the carbon of the acetyl group. Compound **1** was conclusively identified as taraxasteryl acetate, consistent with previous reports [23]. Recently, taraxesteryl acetate showed notable anti-inflammatory effects in a mouse ear edema model induced by chemicals such as phorbol-12-myristate-13-acetate and croton oil [24]. Besides, taraxasterol, a precursor of taraxesteryl acetate, significantly reduced the production of NO, PGE2, TNF-α, interleukin-1β (IL-1β), and IL-6 in LPS-stimulated RAW264.7 macrophages, with effects dependent on the dose [25]. However, no studies have examined the anti-inflammatory effects of taraxesteryl acetate on RAW264.7 macrophages, and this study was limited by the inadequate weight of isolated taraxesteryl acetate, which fell short of the experimental requirements.

The FTIR spectrum of compound **2** revealed distinct absorption bands that aid in understanding its molecular structure. The broad peak at 3195 cm^{-1} indicates an O–H stretching vibration. A strong absorption band at 1666 cm^{-1} suggests a carbonyl group, likely a ketone or aldehyde, while the peak at 1279 cm^{-1} corresponds to a C–O stretching vibration, indicating the presence of an ether or ester functional group (Fig. S7). The ^{1}H-NMR spectrum displayed signals for two *singlet* signals of aromatic protons at δ_H 6.78 and 6.74 ppm. Doublet signals at δ_H 6.16 and 7.86 ppm with J = 9.6 Hz also displayed two aromatic protons (Fig. S8–S9). The ^{13}C-NMR spectrum indicated the presence of a carbonyl group at δ_C 160.7 ppm, four signals of carbons of the aromatic ring: δ_C 112.3, 111.5, 110.7, and 102.6 ppm, in there, signals at δ_C 150.4 and 148.5 ppm is an oxygenated quaternary carbon group (Fig. S10–S11). From the above evidence and in comparison with the NMR data, the structure of compound **2** was elucidated as esculetin [26]. Recent research indicates that esculetin effectively suppresses inflammation by targeting key signaling pathways, particularly the nuclear factor κ-B (NF-κB) and mitogen-activated protein kinase (MAPK) pathways. By lowering critical proinflammatory molecules such as TNF-α, IL-1β, and IL-6, esculetin significantly mitigates the inflammatory response [27-29]. As described in Fig. 3, esculetin at 4 µg/mL (20 µM) inhibited NO production by 22%, similar to prior research showing an IC_{50} of 34 µM in RAW264.7 macrophages [30].

The ^{1}H-NMR spectrum revealed resonance signals for two protons from secondary amine groups at δ_H 11.04 (2H, *brs*), as well as two protons from a conjugated double

bond in an aromatic ring at δ_H 7.36 and 5.49 ppm with doublet signals (J = 7.6 Hz). The ^{13}C-NMR spectrum displayed signals for four carbons: two quaternary carbons at δ_C 166.2 and 153.0 ppm and two olefinic methine groups at δ_C 143.8 and 101.7 ppm. This one-bond pairing indicated a proton bound to one sp^2-hybridized aromatic carbon. The resonance at δ_H 7.36 ppm likewise showed a one-bond correlation with δ_C 143.8 ppm, consistent with a proton attached to a more de-shielded aromatic carbon center (Fig. S12–S13). Additionally, the HSQC and HMBC spectra further clarified long-range connectivity (Fig. S14–S17). The proton at δ_H 5.49 ppm exhibited three-bond couplings to δ_C 143.8 ppm (C6) and to δ_C 166.2 ppm (C4), confirming its spatial proximity to the conjugated carbonyl moiety (C4). Meanwhile, the proton at δ_H 7.36 ppm displayed two-bond and three-bond correlations to δ_C 101.7 (C5), 153.0 (C2), and 166.2 ppm (C4). Utilizing the HMBC and HSQC spectra, the structure of compound **3** has been identified as pyrimidine-2,4-dione (another name is uracil), consistent with a previous report [31]. Additionally, 50 µM pyrimidine-2,4-dione did not significantly inhibit NO production in RAW264.7 macrophages, indicating that higher doses may be required. Conversely, our result indicated that pyrimidine-2,4-dione at 4 µg/mL (about 35 µM) decreased nitric oxide levels by 16% compared to the LPS-stimulated group (Fig. 3).

The FTIR spectrum of compound **4** revealed characteristic stretching peaks at 3106 (N–H), 1692 (C=O), 3221 (O–H), 1280 (C–O), and 2924 cm^{-1} (Csp^2). The presence of both N–H and C=O stretching peaks in the amide region (1600–1700 cm^{-1}) is indicative of a secondary amide. Additionally, the broad O–H stretching peak suggests the presence of an alcohol or phenol group (Fig. S18). The ^{1}H-NMR spectrum showed signals at δ_H 5.17 ppm, a signal of protons oxymethylene, and bonded with the secondary amine (electron-attracting) group. Signals at δ_H 2.48, 2.37, 2.19, and 2.03 ppm related to two methylene groups (Fig. S19–S20). The ^{13}C-NMR spectrum showed one signal at δ_C 181.4 ppm of C=O group (Fig. S20–S21). This evidence, along with the comparison of spectral data from a previous study, confirmed that compound **4** is 5-hydroxypyrrolidin-2-one [32]. To the best of our knowledge, the anti-inflammatory potential of compound **4** has yet to be thoroughly explored. Initial screening revealed that compound **4** at 16 µg/mL reduced NO production by about 37%, with an estimated IC_{50} value of approximately 47.70 ± 3.18 µg/mL (data not shown). Remarkably, pyrrolidine and fused analogs were reported as potential agents for anti-inflammatory, anti-cancer, antiviral, and antituberculosis [33]. Thus, this hypothesis further supports evidence of its anti-inflammatory activity. Taken together, our findings suggest that the presence of active substances plays a significant role in the diverse bioactive activities associated with the inflammatory response.

■ CONCLUSION

The isolation of four natural compounds from *L. sarmentosa* has provided valuable insights into its chemical composition and therapeutic potential. Through advanced spectroscopic techniques, the structural elucidation of taraxasteryl acetate (**1**), esculetin (**2**), pyrimidine-2,4-dione (**3**), and 5-hydroxypyrrolidin-2-one (**4**) revealed that all compounds are identified for the first time in this species. Additionally, the anti-inflammatory effects of these compounds were assessed in LPS-stimulated RAW264.7 macrophages, revealing that compounds **2**, **3**, and **4** significantly inhibited NO production and reduced TNF-α expression. These findings enhance our understanding of anti-inflammatory properties of *L. sarmentosa* and suggest further exploration of its medicinal potential.

■ ACKNOWLEDGMENTS

We sincerely thank Professor Kaeko Kamei from the Kyoto Institute of Technology for providing experimental materials. This work was supported by the Ministry of Education and Training (No. B2023-TCT-21).

■ CONFLICT OF INTEREST

There are no conflicts to declare.

■ AUTHOR CONTRIBUTIONS

Khang Thanh Vo: Writing – original draft, Formal analysis, Investigation, Methodology, Data curation, Writing – review & editing. Cua Dinh Duong:

Investigation, Conceptualization, Formal analysis. Toan Phu Huynh: Investigation, Conceptualization, Formal analysis. Lieu Thi Thuy Ca: Investigation, Conceptualization, Visualization. Giao Huynh Dang: Investigation, Conceptualization, Validation. Thanh Quoc Chau Nguyen: Writing – original draft, Supervision, Resources, Methodology, Conceptualization, Data curation, Writing – review & editing.

■ REFERENCES

[1] Shubhangi, K., Jadhav, R.S., and Vikhe, S.R., 2022, Phytochemical and pharmacological activities of *Launaea sarmentosa*: A review, *Res. J. Pharmacogn. Phytochem.*, 14 (2), 132–135.

[2] Nguyen, T.Q.C., Binh, T.D., Kusunoki, R., Pham, T.L.A., Nguyen, Y.D.H., Nguyen, T.T., Kanaori, K., and Kamei, K., 2020, Effects of *Launaea sarmentosa* extract on lipopolysaccharide-induced inflammation via suppression of NF-κB/ MAPK signaling and Nrf2 activation, *Nutrients*, 12 (9), 2586.

[3] Gunde, M.C., Wani, J.S., and Pethe, A.M., 2022, Pharmacognostic and phytochemical studies on leaves of *Launaea sarmentosa* (Willd.) Schultz - Bip. Ex Kuntze, *Int. J. Ayurvedic Med.*, 13 (3), 759–763.

[4] Das, S., Priyanka, K.R., Prabhu, K., Vinayagam, R., Rajaram, R., and Kang, S.G., 2024, Anticandidal properties of *Launaea sarmentosa* among the salt marsh plants collected from Palk Bay and the Gulf of Mannar Coast, Southeastern India, *Antibiotics*, 13 (8), 748.

[5] Tran, D.Q., Pham, A.C., Nguyen, T.T.T., Vo, T.C., Vu, H.D., Ho, G.T., and Mohsin, S.M., 2024, Growth, physiological, and biochemical responses of a medicinal plant *Launaea sarmentosa* to salinity, *Horticulturae*, 10 (4), 388.

[6] Nguyen, T.Q.C., Hong, T.T., Khang, V.T., Ho, T.N.Y., Pham, D.T., Giao, D.H., Tu, T.T.T., and Kamei, K., 2024, Anti-inflammatory constituents isolated from *Launaea sarmentosa* against infection by LPS-stimulated macrophages, *Rec. Nat. Prod.*, 18 (6), 663–673.

[7] Raju, G.S., RahmanMoghal, M.M., Hossain, M.S., Hassan, M., Bilah, M., Ahamed, S.K., and Rana, M., 2014, Assessment of pharmacological activities of two medicinal plant of Bangladesh: *Launaea sarmentosa* and *Aegialitis rotundifolia* Roxb in the management of pain, pyrexia, and inflammation, *Biol. Res.*, 47 (1), 55.

[8] Nigam, M., Mishra, A.P., Deb, V.K., Dimri, D.B., Tiwari, V., Bungau, S.G., Bungau, A.F., and Radu, A.F., 2023, Evaluation of the association of chronic inflammation and cancer: Insights and implications, *Biomed. Pharmacother.*, 164, 115015.

[9] Novoa, C., Salazar, P., Cisternas, P., Gherardelli, C., Vera-Slazar, R., Zolezzi, J.M., and Inestrosa, N.C., 2022, Inflammation context in Alzheimer's disease, a relationship intricate to define, *Biol. Res.*, 55 (1), 39.

[10] Lee, J.W., Chun, W., Lee, H.J., Min, J.H., Kim, S.M., Seo, J.Y., Ahn, K.S., and Oh, S.R., 2021, The role of macrophages in the development of acute and chronic inflammatory lung diseases, *Cells*, 10 (4), 897.

[11] Oishi, Y., and Manabe, I., 2018, Macrophages in inflammation, repair and regeneration, *Int. Immunol.*, 30 (11), 511–528.

[12] Ahsan, H., Ayub, M., Irfan, H.M., Saleem, M., Anjum, I., Haider, I., Asif, A., Abbas, S.Q., and ul Hulassan, S.S., 2023, Tumor necrosis factor-alpha, prostaglandin-E2 and interleukin-1β targeted anti-arthritic potential of fluvoxamine: Drug repurposing, *Environ. Sci. Pollut. Res.*, 30 (6), 14580–14591.

[13] Singh, J., Lee, Y., and Kellum, J.A., 2022, A new perspective on NO pathway in sepsis and ADMA lowering as a potential therapeutic approach, *Crit. Care*, 26 (1), 246.

[14] Wilmes, V., Scheiper, S., Roehr. W., Niess, C., Kippenberger, S., Steinhorst, K., Verhoff, M.A., and Kauferstein, S., 2020, Increased inducible nitric oxide synthase (iNOS) expression in human myocardial infarction, *Int. J. Legal Med.*, 134 (2), 575–581.

[15] Zamora, R., Vodovotz, Y., and Billiar, T.R., 2000, Inducible nitric oxide synthase and inflammatory diseases, *Mol. Med.*, 6 (5), 347–373.

[16] Lee, M., Rey, K., Besler, K., Wang, C., and Choy, J., 2017, Immunobiology of nitric oxide and

regulation of inducible nitric oxide synthase, *Results Probl. Cell Differ.*, 62, 181–207.

[17] Liao, W., Ye, T., and Liu, H., 2019, Prognostic value of inducible vitric oxide synthase (iNOS) in human cancer: A systematic review and meta-analysis, *BioMed Res. Int.,* 2019 (1), 6304851.

[18] Shah, V., Lyford, G., Gores, G., and Farrugia, G., 2004, Nitric oxide in gastrointestinal health and disease, *Gastroenterology,* 126 (3), 903–913.

[19] Watanabe, S., Alexander, M., Misharin, A.V., and Budinger, G.R.S., 2019, The role of macrophages in the resolution of inflammation, *J. Clin. Invest.*, 129 (7), 2619–2628.

[20] Yan, W., Yan, Y., Luo, X., Dong, Y., Liang, G., Miao, H., Huang, Z., and Jiang, H., 2024, Lipopolysaccharide (LPS)-induced inflammation in RAW264.7 cells is inhibited by microRNA-494-3p via targeting lipoprotein-associated phospholipase A2, *Eur. J. Trauma Emerg. Surg.*, 50 (6), 3289–3298.

[21] Lee, S.J., Lee, U.S., Kim, W.J., and Moon, S.K., 2011, Inhibitory effect of esculetin on migration, invasion and matrix metalloproteinase-9 expression in TNF-α-induced vascular smooth muscle cells, *Mol. Med. Rep.*, 4 (2), 337–341.

[22] Liu, C., Lei, S., Cai, T., Cheng, Y., Bai, J., Fu, W., and Huang, M., 2023, Inducible nitric oxide synthase activity mediates TNF-α-induced endothelial cell dysfunction, *Am. J. Physiol. Cell Physiol.*, 325 (3), C780–C795.

[23] Lee, S., Han, S., Kim, H.M., Lee, J.M., Mok, S.Y., and Lee, S., 2011, Isolation and identification of phytochemical constituents from *Taraxacum coreanum*, *J. Korean Soc. Appl. Biol. Chem.*, 54 (1), 73–78.

[24] Pérez-García, F., Marín, E., Parella, T., Adzet, T., and Cañigueral, S., 2005, Activity of taraxasteryl acetate on inflammation and heat shock protein synthesis, *Phytomedicine*, 12 (4), 278–284.

[25] Zhang, X., Xiong, H., and Liu, L., 2012, Effects of taraxasterol on inflammatory responses in lipopolysaccharide-induced RAW264.7 macrophages, *J. Ethnopharmacol.*, 141 (1), 206–211.

[26] Zhao, C.N., Yao, Z.L., Yang, D., Ke, J., Wu, Q.L., Li, J.K., and Zhou, X.D., 2020, Chemical constituents from *Fraxinus hupehensis* and their antifungal and herbicidal activities, *Biomolecules*, 10 (1), 74.

[27] Wang, F., Jia, Q.W., Yuan, Z.H., Lv, L.Y., Li, M., Jiang, Z.B., Liang, D.L., and Zhang, D.Z., 2019, An anti-inflammatory C-stiryl iridoid from *Camptosorus sibiricus* Rupr., *Fitoterapia*, 134, 378–381.

[28] Hu, J., Zhao, L., Li, N., Yang, Y., Qu, T., Ren, H., Cui, X., Tao, H., Chen, Z., and Peng, Y., 2022, Investigation of the active ingredients and pharmacological mechanisms of *Porana sinensis* Hemsl. against rheumatoid arthritis using network pharmacology and experimental validation, *PLoS One*, 17 (3), e0264786.

[29] Xiu, Z., Li, Y., Fang, J., Han, J., Li, S., Li, Y., Yang., X., Song, G., Li, Y., Jin, N., Zhu, Y., Sun, L., and Li, X., 2023, Inhibitory effects of esculetin on liver cancer through triggering NCOA4p-mediation ferritinophagy *in vivo* and *in vitro*, *J. Hepatocell. Carcinoma,* 10, 611–629.

[30] Li, H., Lin, J., Bai, B., Bo, T., He, Y., Fan, S., and Zhang, J., 2023, Study on purification, identification and antioxidant of flavonoids extracted from *Perilla* leaves, *Molecules*, 28 (21), 7273.

[31] El-Dien, O.G., Shawky, E., Aly, A.H., Abdallah, R.M., and Abdel-Salam, N.A., 2014, Phytochemical and biological investigation of *Spergularia marina* (L.) Griseb. growing in Egypt, *Nat. Prod. Sci.*, 20 (3), 52–159.

[32] Staubmann, R., Schubert-Zsilavecz, M., Hiermann, A., and Kartnig, T., 1999, A complex of 5-hydroxypyrrolidin-2-one and pyrimidine-2,4-dione isolated from *Jatropha curcas*, *Phytochemistry*, 2 (26), 237–238.

[33] Jeelan Basha, N., Basavarajaiah, S.M., and Shyamsunder, K., 2022, Therapeutic potential of pyrrole and pyrrolidine analogs: An update, *Mol. Diversity*, 26 (5), 2915–2937.